

# Bachelorarbeit

eingereicht an der

Fakultät für Physik

der

Ludwig-Maximilians-Universität München



---

## Anodic Oxidation Nanolithography with Atomic Force Microscope

## Anodische Oxidation Nanolithografie mit dem Rasterkraftmikroskop

---

Klara Werder

Betreuer:

Prof. Dr. Dmitri K. Efetov

Oktober, 2023



# 1 Contents

2	Abstract.....	2
3	Background.....	2
3.1	Graphene.....	2
3.1.1	Bilayer graphene .....	4
3.2	Van der Waals Heterostructures .....	5
3.2.1	Hexagonal Boron Nitride/graphene devices .....	5
3.3	Fabrication.....	6
3.3.1	Exfoliation.....	6
3.3.2	Flake Identification .....	6
3.3.3	Stacking Procedure.....	7
3.4	Atomic force microscope.....	8
3.4.1	Modes.....	9
3.4.2	Anodic oxidation cutting.....	10
4	Cutting Graphite with AFM.....	11
4.1	Testing out Parameters .....	13
4.1.1	Humidity.....	13
4.1.2	Drive2 Amplitude (Lock-In2) .....	14
4.1.3	Z distance (Connect) .....	16
4.1.4	XY velocity (Connect) .....	16
4.2	Patterns .....	17
4.2.1	AutoCAD patterns and implementing in NanoMan.....	17
4.2.2	Testing out Patterns .....	19
4.3	Picking up and dropping after AFM cutting.....	21
5	Conclusion and Outlook .....	23
6	Bibliography .....	24

## 2 Abstract

After the discovery of graphene in 2004 the field of two dimensional materials grew. The need of improving devices and with it better cleanliness of a device led to new discoveries. Here a new method of nanolithography, which allows patterning in the range of 100 nm, is presented.

## 3 Background

### 3.1 Graphene

Two dimensional (2D) materials are one atomic layer of three dimensional (3D) materials. They were thought of to not exist other than as an integral part of a 3D material. That was until in 2004 Novoselov et al. discovered graphene.<sup>1</sup> Graphene is a single atomic layer of graphite and made out of carbon atoms. They arrange themselves in a honeycomb structure made of hexagons. (Figure 1) This structure is not a Bravais lattice, so we think of it as a triangular lattice with a basis of two atoms, A and B, per unit cell. The lattice vectors can be written as

$$a_1 = \frac{a}{2}(3, \sqrt{3}), \quad a_2 = \frac{a}{2}(3, -\sqrt{3}), \quad (1)$$

where  $a \approx 1.42 \text{ \AA}$  is the carbon-carbon distance. The reciprocal lattice is also a hexagon. The reciprocal lattice vectors are given by

$$b_1 = \frac{2\pi}{3a}(1, \sqrt{3}), \quad b_2 = \frac{2\pi}{3a}(1, -\sqrt{3}). \quad (2)$$

The points  $K$  and  $K'$  at the corners of the graphene Brillouin zone (BZ) also called the Dirac points are found when defining the first BZ. Their positions in momentum space are given by

$$K = \left(\frac{2\pi}{3a}, \frac{2\pi}{3\sqrt{3}a}\right), \quad K' = \left(\frac{2\pi}{3a}, -\frac{2\pi}{3\sqrt{3}a}\right). \quad (3)$$

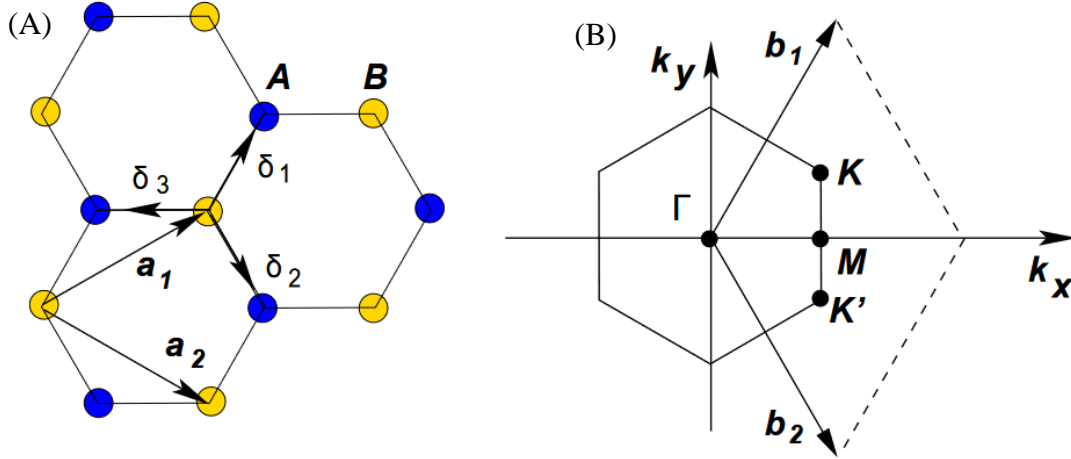


Figure 1: (A) Graphene lattice structure with two sublattices A and B and lattice vectors  $a_1$  and  $a_2$  (B) Brillion zone and Dirac points K and K'.<sup>2</sup>

The Dirac points are of great importance in the electronic transport of graphene. They play a role like the role of  $\Gamma$  points in direct bandgap semiconductors. The tight binding Hamiltonian for electrons in graphene, considering that electrons can hop both to nearest and next nearest neighbour atoms, is given by

$$H = -t \sum_{\langle i,j \rangle, \sigma} (a_{\sigma}^{\dagger} b_{\sigma,j} + h.c.) - t' \sum_{\langle\langle i,j \rangle\rangle, \sigma} (a_{\sigma,i}^{\dagger} a_{\sigma,j} + b_{\sigma,i}^{\dagger} b_{\sigma,j} + h.c.) \quad (4)$$

where  $a_{i,\sigma}$  ( $a_{i,\sigma}^{\dagger}$ ) annihilates an electron with spin  $\sigma$  ( $\sigma = \uparrow, \downarrow$ ) on site  $R_i$  on sublattice A. For sublattice B an equivalent definition is used.  $t$  ( $\approx 2.8$  eV) is the nearest neighbour hopping energy, which translates to hopping between different sublattices,  $t'$  is the next nearest neighbour hopping energy, that is hopping in the same sublattice. The energy bands derived from this Hamiltonian have the form

$$E_{\pm}(k) = \pm t \sqrt{3 + f(k)} - t' f(k), \quad (5)$$

$$f(k) = 2 \cos(\sqrt{3} k_y a) + 4 \cos\left(\frac{\sqrt{3}}{2} k_y a\right) \cos\left(\frac{3}{2} k_x a\right),$$

where the plus sign applies to the upper ( $\pi$ ) and the minus sign to the lower ( $\pi^*$ ) band. The band structure for small  $q$  relative to the Dirac points K (or K') is given by

$$E_{\pm}(q) \approx \pm \hbar v_F q + O((q/k)^2) \quad (6)$$

where  $\hbar$  is the reduced Planck's constant,  $q$  is the momentum measured relative to the Dirac points and  $v_F$  represents the fermi velocity. (Figure 2) Therefore, graphene is a zero bandgap semiconductor with a linear wavelength energy dispersion for both electrons and holes in the conduction and valence bands. When intervalley scattering is neglected ( $t' = 0$ ) both Dirac cones have the same dispersion, and all properties can be studied near the  $K$  point accounting for the  $K'$  point with an extra valley degeneracy  $g_v = 2$ . Therefore, due to double spin and double valley degeneracy graphene bands are 4 fold degenerate.<sup>2,3</sup> This degeneracy has been confirmed in quantum Hall effect experiments.<sup>4,5</sup> The linear dispersion of the Dirac cones also leads to electrons behaving as massless Dirac electrons. Which leads to showing an anomalous Hall effect in experiments and realizing experimental proposals on relativistic particles such as Klein tunnelling.<sup>4-7</sup>

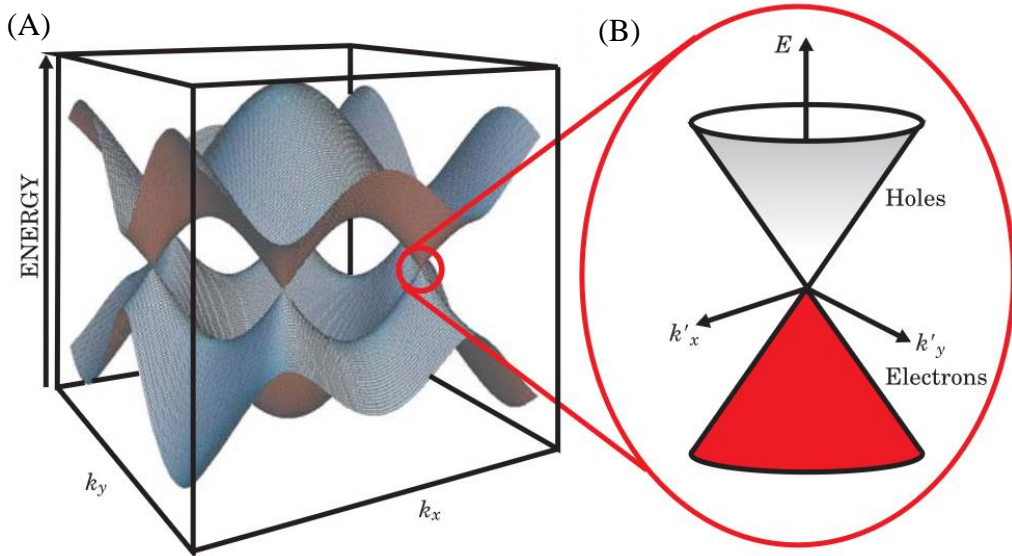


Figure 2: (A) Band structure of graphene (B) zoom in on K or K' point.<sup>3</sup>

### 3.1.1 Bilayer graphene

Bilayer graphene are two graphene monolayers that are weakly coupled. It is usually in the AB stacking, which is the 3D graphite stacking. AB stacking refers to half of the top layer atoms laying in the vacancies of the bottom layer. Bilayer graphene is a gapless semiconductor with parabolic dispersion relation. Its bandgap can be opened by applying a displacement field in vertical direction.<sup>3,8</sup> Bilayer graphene can have a twist angle, which can happen naturally. Due to a twist a moiré pattern can be seen and can be directly measured in scanning tunnelling microscope (STM) experiments.<sup>9</sup> In 2011 it was theoretically reported that at certain twist

angles, magic angles, the Dirac point velocity vanishes, accompanied by a very flat Moiré band. This contributes a sharp peak to the Dirac point density of states.<sup>10</sup> In 2018 samples near one magic angle  $\theta_{magic} \approx 1.1^\circ$  were fabricated. They found insulator states at half filling and superconductivity states slightly doped away from the insulator states.<sup>11,12</sup> After that more groups started fabricating twisted bilayer graphene devices. For example in 2023 a gate defined symmetry-broken Josephson junctions in magic-angle twisted bilayer graphene devices was fabricated, with a gate with a  $\sim 150$  nm wide cut in it.<sup>13</sup>

## 3.2 Van der Waals Heterostructures

The discovery of graphene gave rise to the discovery of other 2D materials, which can be combined in Van der Waals (VDW) heterostructures. VDW heterostructures are structures combining two types of materials with dissimilar chemical compositions, lattice structures, or electronic properties by VDW force. VDW interaction is a universal intermolecular force including dipole-dipole, dipole-induced dipole, and induced dipole-induced dipole interactions. The VDW force is generally weaker than typical chemical bonds. Two dimensional heterostructures are of great interest. They opened new opportunities for creating artificial materials by the ability to vary the twist angle between the atomic layers. But it is a challenge to keep the heterostructure contact clean for realizing the designed electronic functions between the materials in it. By trying to create high quality graphene devices hexagonal boron nitride (hBN) came in to play and with it one of the earliest 2D heterostructures. hBN was explored as a substrate and encapsulation layer to form graphene/hBN heterostructures.<sup>14</sup>

### 3.2.1 Hexagonal Boron Nitride/graphene devices

hBN is a wide bandgap insulator. It has a similar structure to graphene in the form of a hexagonal lattice. It has alternating B and N atoms with an AA sequencing stacking bounded by VDW forces. AA sequencing means each boron atom is sandwiched between two nitrogen atoms in the adjacent layers and vice versa. hBN/graphene heterostructures allowed deep insights into intrinsic graphene physics in terms of quantum Hall effects and tunability of its optoelectronic properties by inducing secondary Dirac points or new plasmonic states. hBN used as an alternative gate dielectric compared to SiO<sub>2</sub> improved the properties leading to ballistic transport with a large negative transfer resistance and the mean free path exceeding  $\sim 3$   $\mu\text{m}$  at low temperature and mobilities of up to  $100,000 \text{ cm}^2 \text{ V}^{-1} \text{ s}^{-1}$  at room temperature.<sup>15-17</sup>

For all devices made, a focus is quality improvement, for example with the use of hBN or the use of graphite as a gate instead of amorphous metal. Gates are used for charge tuning. For devices like the gate defined symmetry-broken Josephson junctions in magic-angle twisted bilayer graphene cuts in the scale of 100 nm are required. This has been made by O<sub>2</sub> etching for now. But atomic force microscopy anodic oxidation nanolithography could be a better alternative.<sup>18</sup>

### 3.3 Fabrication

For a device you must fabricate it. Fabrication of high quality devices requires a few crucial steps. The first steps of fabrication are explained here.

#### 3.3.1 Exfoliation

For exfoliation graphite bulk crystals, scotch tape, and Si/SiO<sub>2</sub> chips as a substrate are needed. At first the Si/SiO<sub>2</sub> chips are being prepared by etching it in an O<sub>2</sub> plasma etcher. This step is used to clean the chips from adsorbates. Then a graphite crystal is placed a few times on the sticky side of a piece of scotch tape to let some part of it stick to it. After removing the rest of the crystal, the tape is folded a few times to spread the graphite on it. With this step the bulk crystal is breaking up into less layers. The Si/SiO<sub>2</sub> Chips with the SiO<sub>2</sub> side first are placed on the tape with graphene and are pressed down. Then the tape plus chips is placed on a hot plate with ca. 100° temperature for a few minutes. By increasing the temperature pressure builds up against the graphite. This leads to gas realising through the edges of the graphite. After removing the tape plus chips from the heater the tape is slowly removed from the chips. In this process the graphite is split apart due to the competition of forces between sticking to the tape and sticking to the chip. Which leads to leaving few layer and monolayer graphene on the chip.

19

For hBN exfoliation the steps are similar. Si/SiO<sub>2</sub> chips have been prepared by O<sub>2</sub> plasma etching. After that the hBN crystals are placed on the scotch tape. Then it is being folded a few times to spread the hBN. Another tape is made from the first tape to thin down the crystal further. The second tape is called daughter tape and one can reuse the first tape, mother tape, for a few times. The etched Si/SiO<sub>2</sub> chips are placed on the daughter tape and are pressed down. The pressing down should be less strong than for graphene. After that the tape plus chips are left like this for a few minutes and then the chips are very slowly removed.

#### 3.3.2 Flake Identification

On the exfoliated chips not only monolayer and few layer graphene are left. Bigger graphite components can be found as well. To find flakes in the right size, one needs to identify them. For flake identification an optical microscope is used. This is a fast and easy method which works well with graphene on Si/SiO<sub>2</sub> chips with SiO<sub>2</sub> thickness of 280 nm. You can see an optical contrast due to an increased optical path and to the notable opacity of graphene. It is looked after the right colour for the respective height of the flake.<sup>20</sup> For the purpose of this work, it is searched after graphite, as gates, of around 10 layers. On an optical microscope, that translates to a dark purple colour. The graphite gates should be around 25 µm in length and 5 µm in width. An easy way to organize the found flakes is to create a PowerPoint. (Figure 3)

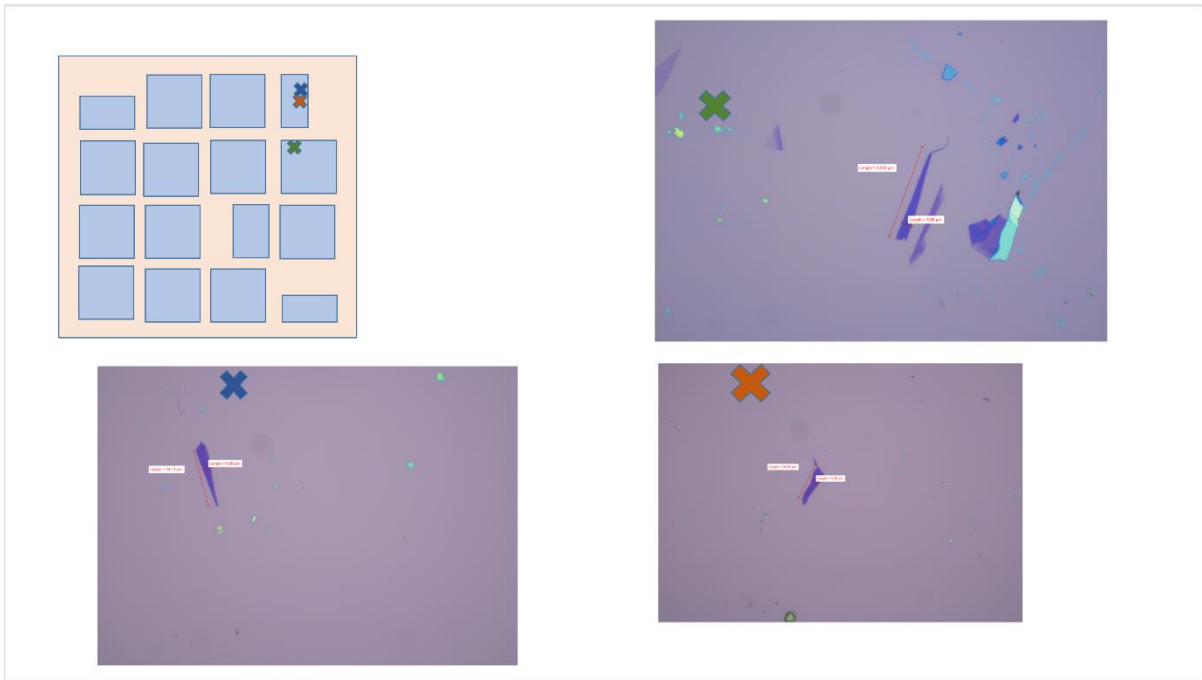


Figure 3: Example of a slide in PowerPoint for sorting found flakes. Example of flake colour.

### 3.3.3 Stacking Procedure

For the stacking procedure a stamp must be made. The stamp consists of a glass plate on which a 0,5 x 0,5 cm polydimethylsiloxane (PDMS) quadrat is placed. The PDMS serves as a cushion material. At last, a polycarbonate (PC) film is placed above the PDMS with scotch tape. (Figure 4) With this stamp picking up hBN and graphite is possible. For that a pickup station with an optical microscope is used. The picking up temperature is at around 110° C and the dropping



Figure 4: Image of a stamp

temperature is at 180° C, at which the PC melts. Directly picking up hBN is easier than directly picking up graphite. Because non etched chips were used in our experiment picking up graphite without hBN was possible.

### 3.4 Atomic force microscope

The atomic force microscope (AFM) is a scanning probe microscope. It scans the surface of a sample with a tip in a grid method. The general structure is shown in Figure 5. It consists of cantilever with a tip and in most cases a laser diode with a corresponding photodiode detector. The tip is typically less than 5  $\mu\text{m}$  tall and often less than 10 nm in diameter at the apex. The cantilever is usually 100–500  $\mu\text{m}$  long. The cantilever bends and deflects caused by forces between the tip and the sample. This motion is detected while the tip is scanning over the sample. To detect the movement, a light beam from the laser diode that reflects off the back of the cantilever into the position sensitive photo detector is used in most cases. A computer generates a map of the surface topography with the measured cantilever deflection. The distance between the tip and the sample plays a role in which type of force will be sensed.

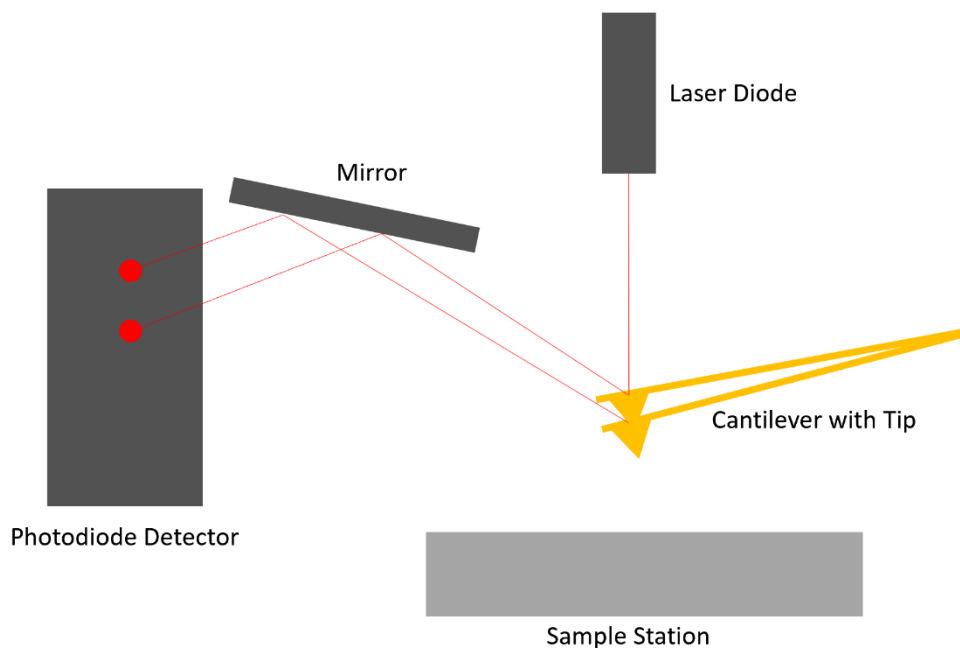


Figure 5: Installation of atomic force microscope.

The forces are sensed depending on the interatomic distance including van der Waals, electrostatic, magnetic, capillary, or ionic repulsion forces. When the tip is getting closer to the sample a weakly attraction, mostly Van der Waals interactions, between their atoms takes place.

But at some point, their electron clouds start to repel each other. This weakens the attraction force until it is just repulsive force.<sup>21,22</sup> (Figure 6)

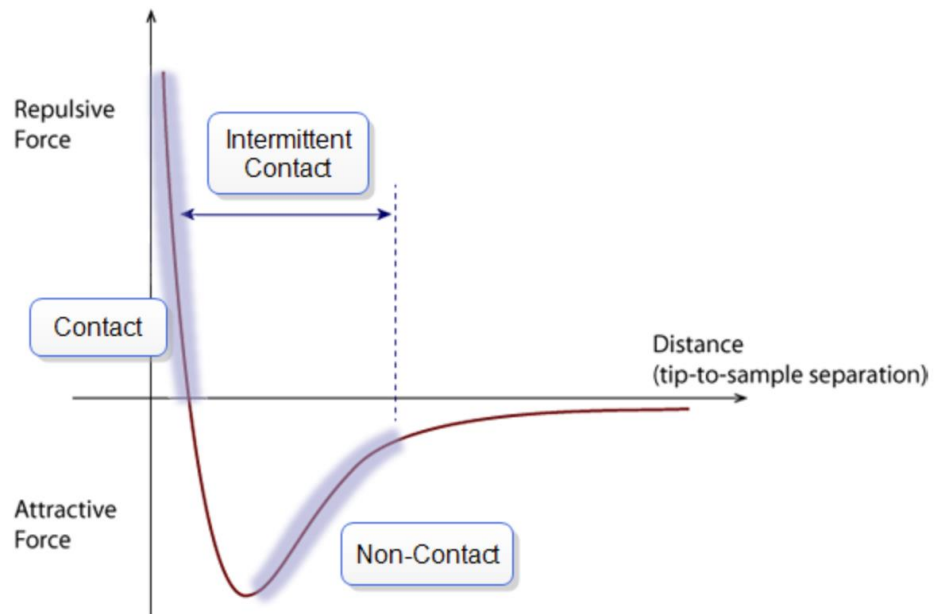


Figure 6: Interatomic force curve between tip and sample.<sup>22</sup>

### 3.4.1 Modes

There are three conventional modes used for AFM, contact mode, non contact mode and tapping mode.

In contact mode, the tip and sample are in close contact during the scanning process. The mode operates in the repulsive region of the interatomic force curve. The cantilever bends because of the contact force in accordance with the topography of the sample. By monitoring, a constant deflection between the cantilever and the sample is kept, so that the force between the tip and the sample is constant.

In the noncontact mode, the tip and cantilever stay at small distance away from the surface, while they are oscillated. The oscillation is in the resonant frequency of the cantilever with amplitude of a few tens to hundreds of Ångstroms. The spacing between the tip and the sample is generally on the order of tens to hundreds of Ångstroms. The interatomic force is in the attractive area of the curve. Changes in frequency are detected and kept constant by adjusting in response to those changes.

In tapping mode, the tip makes repulsive contact with the surface of the sample with an oscillating cantilever. Its oscillation amplitude changes with the sample surface topography, which is monitored. This mode is in the intermitted contact part of the interatomic force curve.

There are other things one can do with an AFM, like using it as a nanolithography technique.<sup>21,22</sup>

### 3.4.2 Anodic oxidation cutting

The anodic oxidation cutting with AFM is a nanolithography technique. It can for example be used to cut different graphite gates. Liam A. Cohen et al. recently cut three different structures, a quantum point contact (QPC), quantum dot array and Fabry–Pérot interferometer, all meant to be operated in the quantum Hall regime.

The general composition of a cutting can be seen in Figure 7. It is started in contact mode, where a conductive tip is brought to the surface in a humid environment. After that it is lifted in tapping mode. Due to capillary forces a water meniscus is formed, connecting the tip and the surface. When a voltage is applied to the tip it catalyses the oxidation. While scanning across the surface a cut is produced.

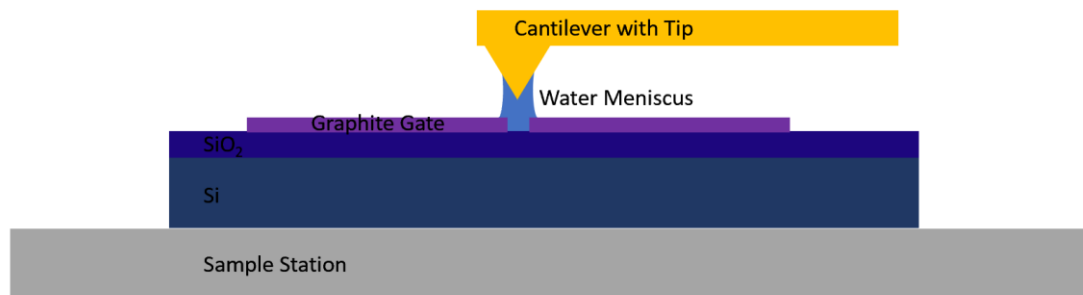
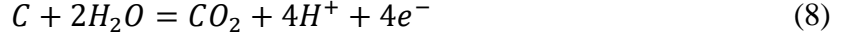


Figure 7: schematic of an anodic oxidation cut.

In the chemical process of oxidation, the carbon is oxidized with water into CO and CO<sub>2</sub> which can be seen in equation (7) and (8).



An ac voltage is used in our experiment. Due to using an ac voltage, which can flow through dielectric substrates in the form of displacement current, instead of a dc voltage no microelectrodes must be attached. This method was introduced in 2018 by Hongyuan Li et al. and makes using AFM nanolithography easier and faster to use.

The voltage drop through the water meniscus  $U_R$  can be calculated as

$$U_R = \frac{R}{R + \frac{1}{j2\pi fC}} U. \quad (9)$$

This is the voltage between the AFM tip and the graphene sample.  $R$  is the water bridge considered as a resistor.  $U$  is the ac voltage applied at the tip.  $\frac{1}{j2\pi fC}$  is the impedance of the graphene/SiO<sub>2</sub>/Si multilayer, that is seen as a capacitor.  $j$  is the imaginary unit,  $C$  is the capacitance and  $f$  is the frequency.

While cutting it can happen that amorphous residue is remaining. They are probably carbon and carbon oxides. In theory these oxide residues should not be picked up, when using the flake in a devise. This is because of the stronger adhesion to the original SiO<sub>2</sub> than to the pickup tool, a stamp, or a stamp with a hBN flake. This self cleaning makes the lithography method a cleaner alternative to O<sub>2</sub> etching.<sup>18,23,24</sup>

## 4 Cutting Graphite with AFM

The cuts are going to be made with Bruker Dimension Icon with Nanoscope Software. The tips used are Nanoworld Arrow NcPt. The tip side and the detector side are coated with Pt/Ir. The tip side coating enhances the conductivity of the AFM tip and allows electrical contacts. The detector side coating enhances the reflectance of the laser beam and prevents light from interfering within the AFM cantilever.<sup>25</sup> We are using graphite flakes of around 10 layers exfoliated on non etched chips.

In the anodic oxidation mode, we start by scanning an image in “scan” (tapping mode). After that we switch to “nanoMan”. (Figure 8 (A)) Here different cutting parameters can be adjusted, and patterns can be implemented. (Figure 8 (B), (C)) For line cuts the path is made directly in

nanoMan. The parameters will be discussed in 4.1 and the patterns in 4.2. For a general cut the parameters used in “Segment” are “XY velocity” at 1  $\mu\text{m/s}$ , “Tip voltage” at 0 V. The “Segment” section stands for how the tip moves in contact mode before and after a cut. For “Connect” the general parameters are “Feedback mode” “off”, “Z distance” at 500 nm, “Z velocity” at 100 nm/s, “XY velocity” at 1  $\mu\text{m/s}$ . The “Connect” section stands for the cutting in tapping mode. (Figure 8 (B)) For the “Lock-In2” the general parameters are “Drive2 Frequency” at 150 kHz, “Drive2 Amplitude” at 10000 mV. In “Lock-In2” the voltage that is applied to the tip is adjusted. (Figure 8 (D)) The humidity is held at 50 %. After making the path the tip must “Move To Path” first. Then the “Drive2 Amplitude” is set to 10000 mV, and we can click on “Do It” for the cut to start. After the cut was made, we withdraw and change the tip to a normal tapping mode tip, here Budget Sensors Tap300AI-G are used. By changing

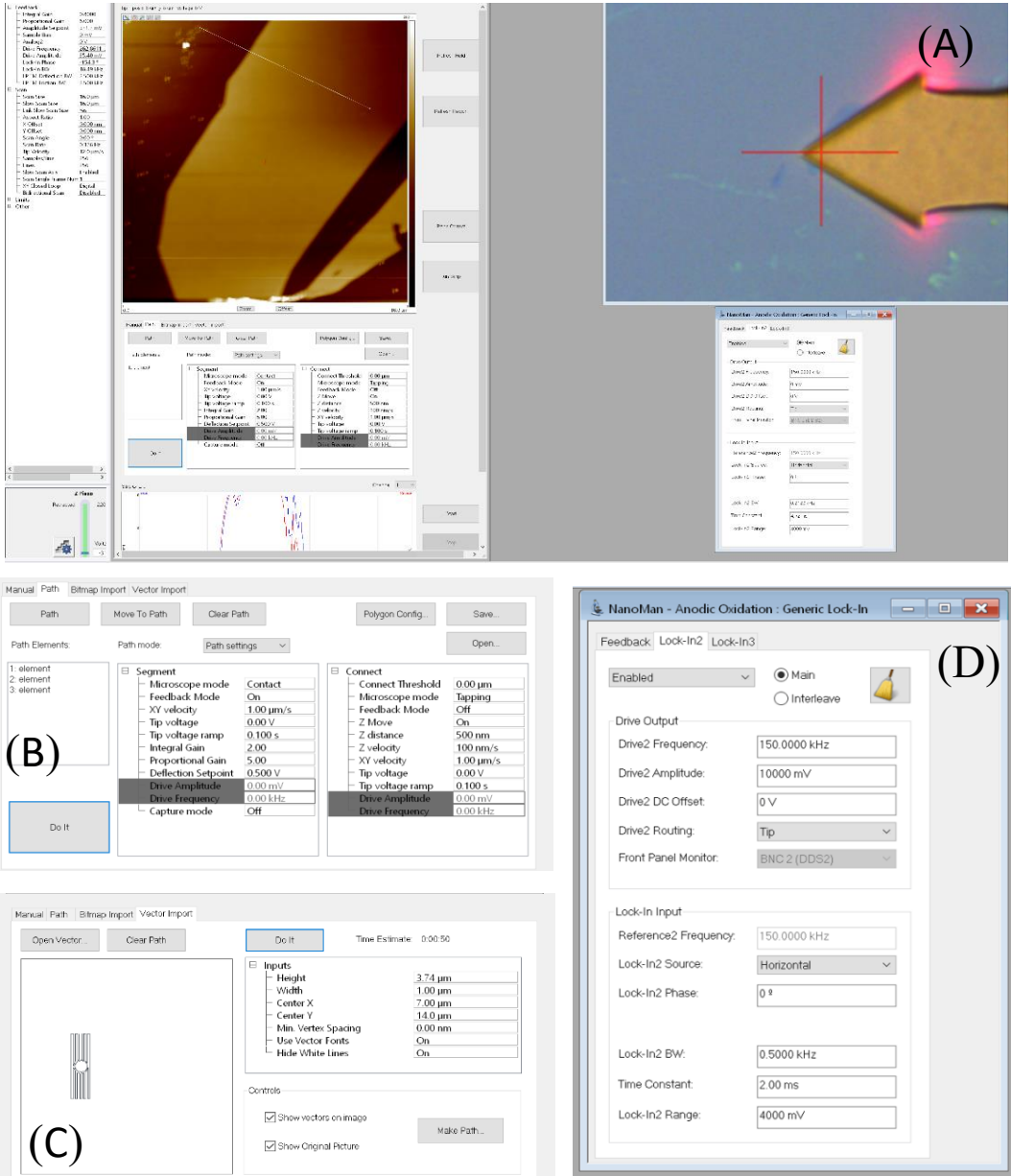


Figure 8: (A) NanoMan page overview (B) Zoom into Path page (C) Zoom into generic lock-In page (D) Zoom into Vector Import page.

to a normal tapping mode tip, the image quality will be increased. With the new tip an image in

standard tapping mode is made to see how the cutting worked. After that it can be analysed in Gwyddion. It can be seen that the cut went completely through the graphite. (Figure 9)

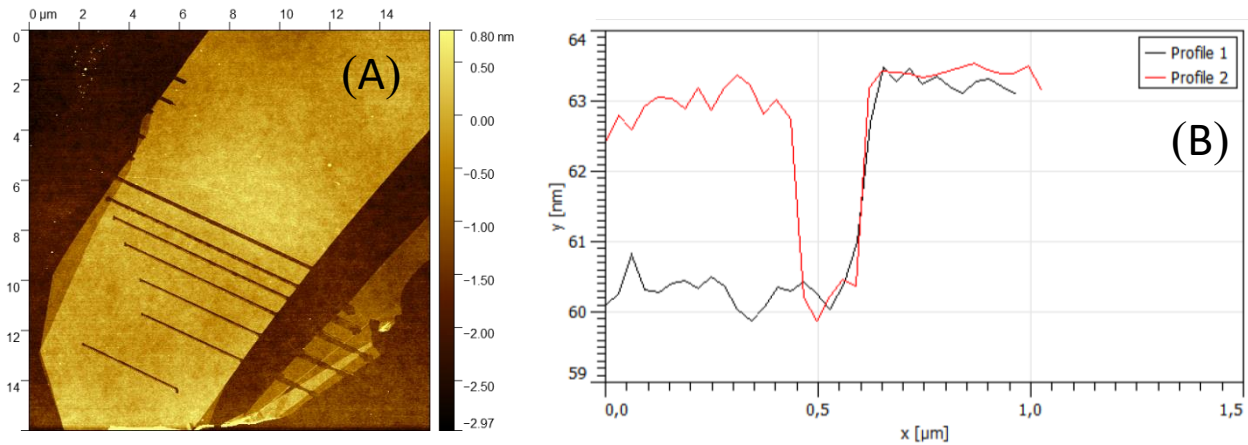


Figure 9: (A) Image after cutting (B) Image of height graph. Profile 1 is the height difference between the graphite and the chip on the edge of the flake. Profile 2 is the height difference between graphite and the cut.

## 4.1 Testing out Parameters

To get a perfect cut we need the right parameters. We are testing the humidity, Z distance, XY velocity and Drive2 Amplitude. Every parameter except the one tested is kept as the general cutting parameters.

### 4.1.1 Humidity

Humidity plays a big part in making a cut, that is why it was tested out here. We did three test runs in which we started from low humidity to high humidity on graphite gates. To decrease the humidity, pressured nitrogen gas, that is low in humidity, was used. To increase the humidity a hotplate with a glass of water was used.

As can be seen in Figure 10, at higher humidity “bubbles” started to appear. They look like the meniscus expanded in the outside direction in the form of waves. At higher humidity it can also be seen that the cuts get wider. (Figure 11) The width depends also on the tip that is used. After using one tip for a while the tip wears out. It gets less pointy, and the cuts are getting wider.

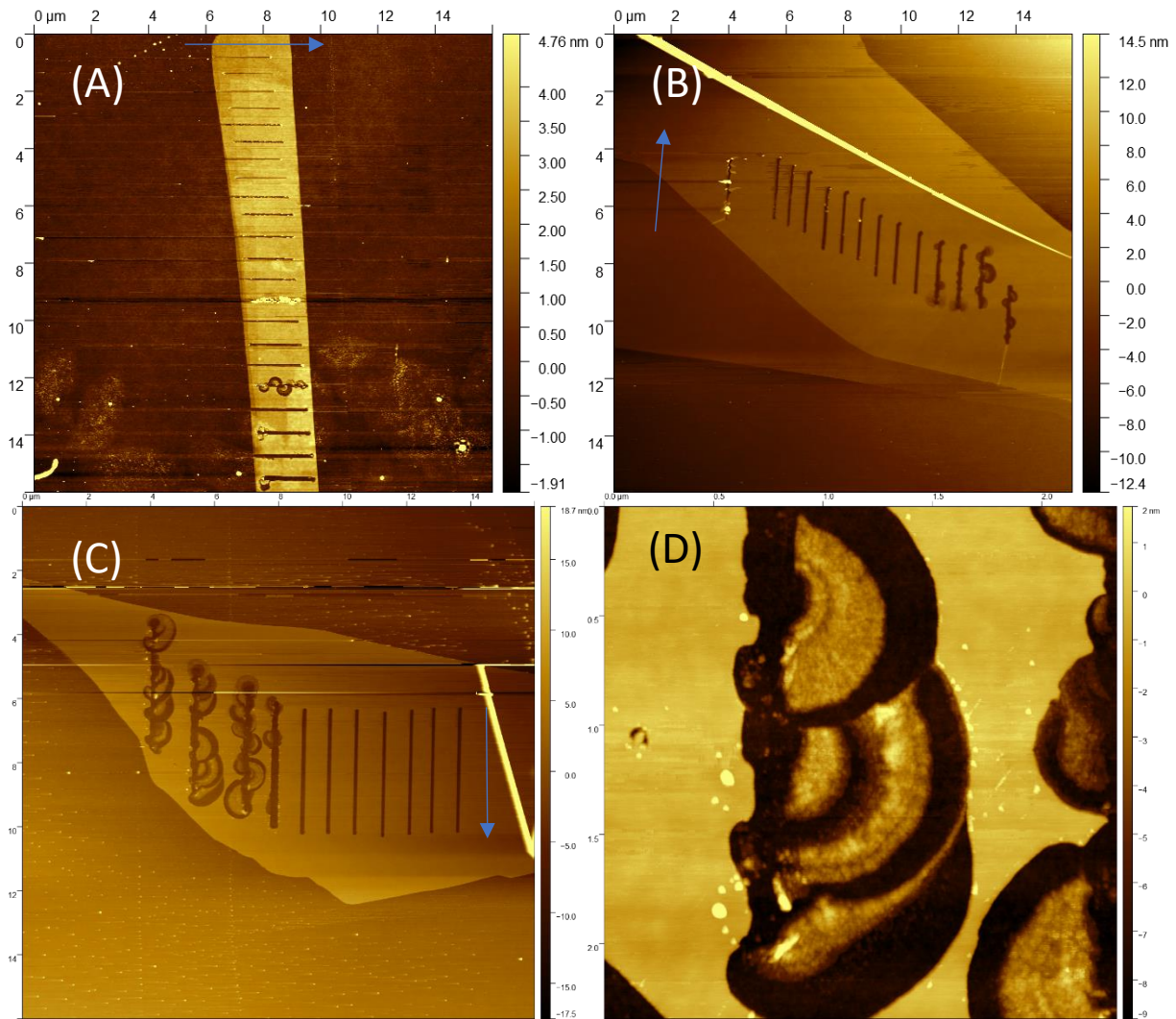


Figure 10: (A) Humidity cuts on graphite flake. The blue arrow shows the cutting direction. Humidity values from up to down: 45 %, 45 %, 46 %, 46 %, 52 %, 52 %, 50 %, 50 %, 54 %, 54 %, 56 %, 56 %, 58 %, 58 %, 62 %, 62 %, 67 %, 67 %, 71 %, 71 %, 75 %, 75 %. (B) Humidity cuts on graphite flake. The blue arrow shows the cutting direction. Humidity values from left to right are: 35 %, 45 %, 47 %, 48 %, 49 %, 49 %, 52 %, 52 %, 55 %, 57 %, 64 %, 68 %, 72 %, 75 %. With two not cut cuts between 35 % and 45 % at 36 % and 44 %. (C) Humidity cuts on graphite flake. The blue arrow shows the cutting direction. Humidity values from left to right are: 79 %, 79 %, 77 %, 75 %, 68 %, 57 %, 56 %, 51 %, 51 %, 48 %, 48 %. (D) Zoom in on bubble of second cut from (C).

#### 4.1.2 Drive2 Amplitude (Lock-In2)

The Drive2 Amplitude is the voltage that is applied to the tip, so this is an important parameter to test out. It was tested from low voltages to high voltages on graphite gates each with twice cuts on the inside of the flake.

For low voltages no clean cuts appear. Only at 9 V and 10 V the cut is good. In the first test it seemingly started to cut at 6 V, but it did not result in a clean cut. On both tests only one of the cuts at 9 V and 10 V was successful. This could be because of dirt on the flake. The cuts do not have a distinct difference in width and depth. For now, we are staying at 10 V to get clean cuts. (Figure 12)

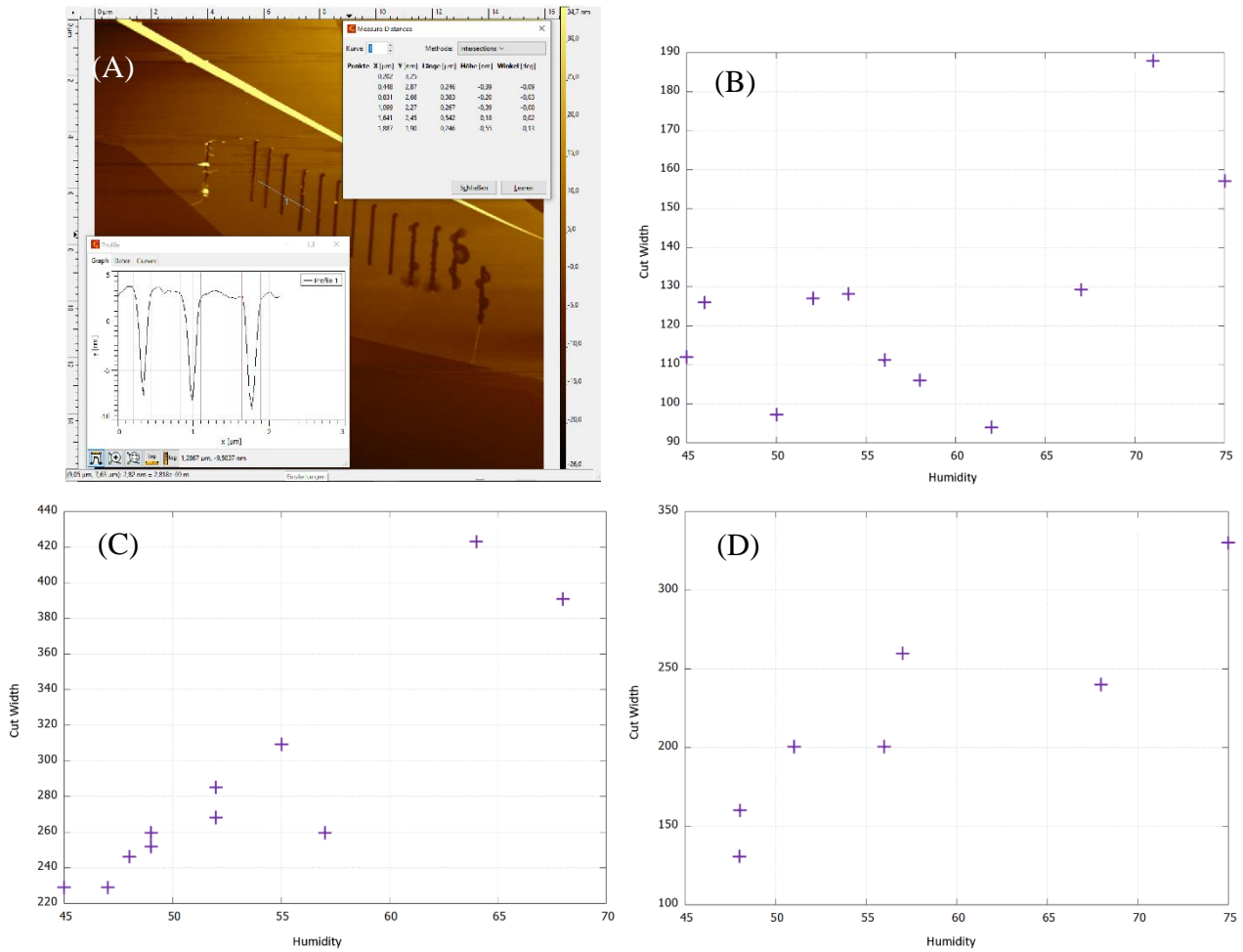


Figure 11: (A) Image of high graph (B) plotted cut width on humidity for first test (C) plotted cut width on humidity for second test (D) plotted cut width on humidity for third test.

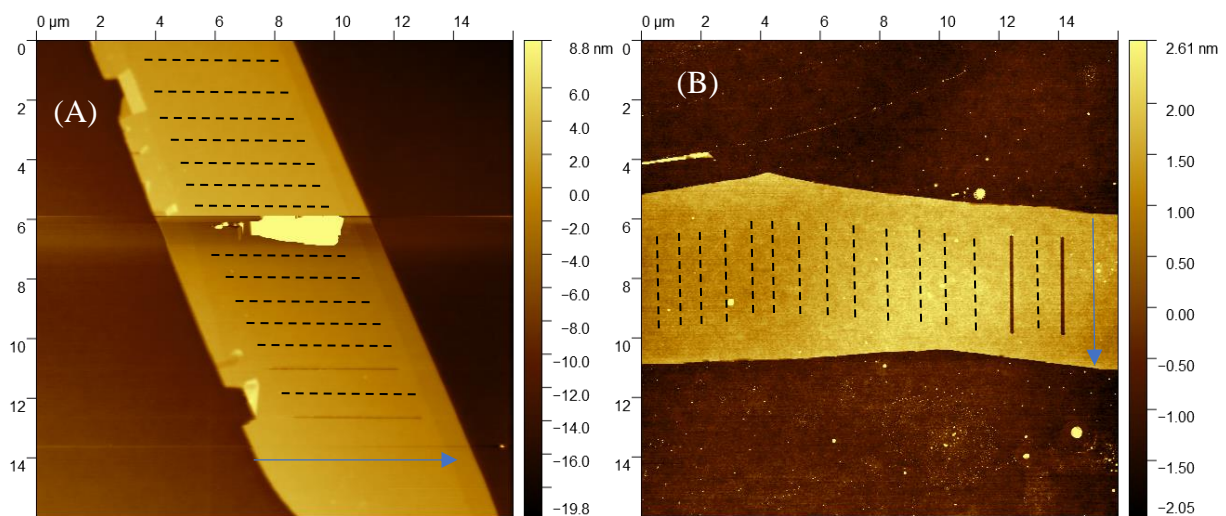


Figure 12: (A) Drive2 Amplitude cuts on graphite flake. Blue arrow shows the cutting direction. Dotted lines show wanted cuts. Drive2 Amplitude values from up to down are: 2 V, 2 V, 4 V, 4 V, 5 V, 5 V, 6 V, 6 V, 7 V, 7 V, 8 V, 8 V, 9 V, 9 V, 10 V, 10 V. (B) Drive2 Amplitude cuts on graphite flake. Blue arrow shows the cutting direction. Dotted lines show wanted cuts. Drive2 Amplitude values from left to right are: 3 V, 3 V, 4 V, 4 V, 5 V, 5 V, 6 V, 6 V, 7 V, 7 V, 8 V, 8 V, 9 V, 9 V, 10 V, 10 V.

### 4.1.3 Z distance (Connect)

The Z distance in the Connect segment is the distance from the sample to the tip while the tip is cutting. It was tested from high distance to low distance each with twice cuts one from the outside of the flake to the inside and one completely in the inside.

The cuts on the inside of the flake did not cut, it only made a point at the end of the expected cut. This could result from dirt on the flake. There is no distinct difference in the width and the depth of the cuts. There is also no clear distribution of how much oxide residue is created. For now, we are staying at the height of 500 nm. (Figure 13)

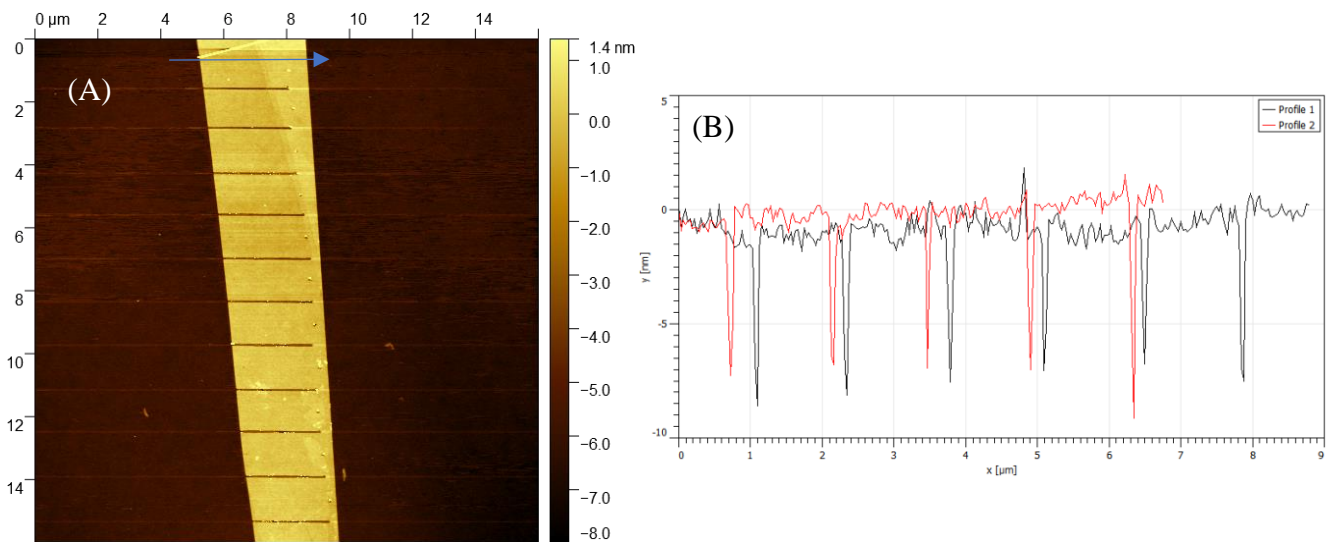


Figure 13: Z distance cuts on graphite gate. Blue arrow shows the cutting direction. Z distance values from up to down are: 900 nm, 800 nm, 700 nm, 600 nm, 500 nm, 400 nm, 300 nm, 200 nm, 100 nm, 450 nm, 550 nm. (B) Height graph of the cut graphite. Profile 1 covers the first 6 cuts. Profile 2 covers the 5 last cuts.

### 4.1.4 XY velocity (Connect)

The XY velocity in the Connect segment is the velocity in which the cuts are made. It was tested from low velocity to high velocity two times with each cut two times per value.

For every value it cuts at least one line. For 4 and 5  $\mu\text{m/s}$  all lines were cut. For not executed cuts at 1 and 3  $\mu\text{m/s}$  it created a point at the end of the expected cut. There is no distinct difference in width or depth between the cuts. The oxide residue has no clear distribution either. (Figure 14)

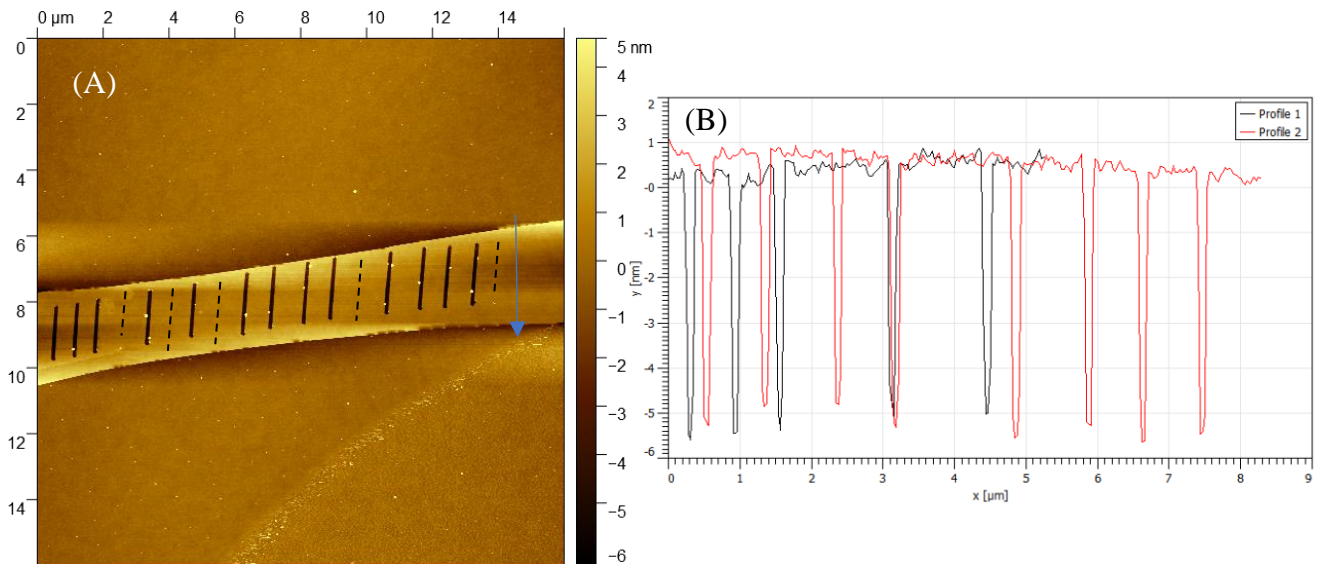


Figure 14: (A) XY velocity cuts on graphite gate. Blue arrow shows the cutting direction. Dotted lines show wanted cuts. XY velocity values from left to right each are: 4 μm /s, 4 μm /s, 3 μm /s, 3 μm /s, 2 μm /s, 2 μm /s, 1 μm /s, 1 μm /s, 5 μm /s, 5 μm /s, 4 μm /s, 4 μm /s, 3 μm /s, 3 μm /s, 2 μm /s, 2 μm /s, 1 μm /s, 1 μm /s. (B) Image of height graph. Profile 1 contains the first 5 cuts. Profile 2 contains the last 8 cuts.

## 4.2 Patterns

For advanced gates, patterns are a must. Here we are testing out what can be made and where the difficulties lay. For the creation of patterns, the software AutoCAD is used.

### 4.2.1 AutoCAD patterns and implementing in NanoMan

AutoCAD is a CAD software application, in which patterns for nanoMan can be easily made.

For a line cutting “Polylinie” or “Kreis” is used. With that, one can draw their desired structure. For area cutting a pattern with a lot of lines next to each other is wanted. For that we estimate one line to be around 90-100 nm in the cutting. To make a pattern like this either “Polylinie” and “Kreis” are used. For that all lines must be drawn by hand, but one connecting line can be made. The alternative is to use hatching. For that the desired area is first outlined by “Polylinie” and “Kreis” after that we use the hatch tool with “line” pattern. The density of lines can be adjusted in “Eigenschaften”. (Figure 15) With this pattern every hatch line is translated as one own line cut in nanoMan. To implement the made patterns in nanoMan, the structure is exported as \*.wmf. In nanoMan we go to the Vector Import section and open the exported vector. The height and width as well as the position are adjusted, and the path is made. After that the path

can be opened in the section “Path”. (Figure 16) The cutting direction of the path can be adjusted by right clicking on it.

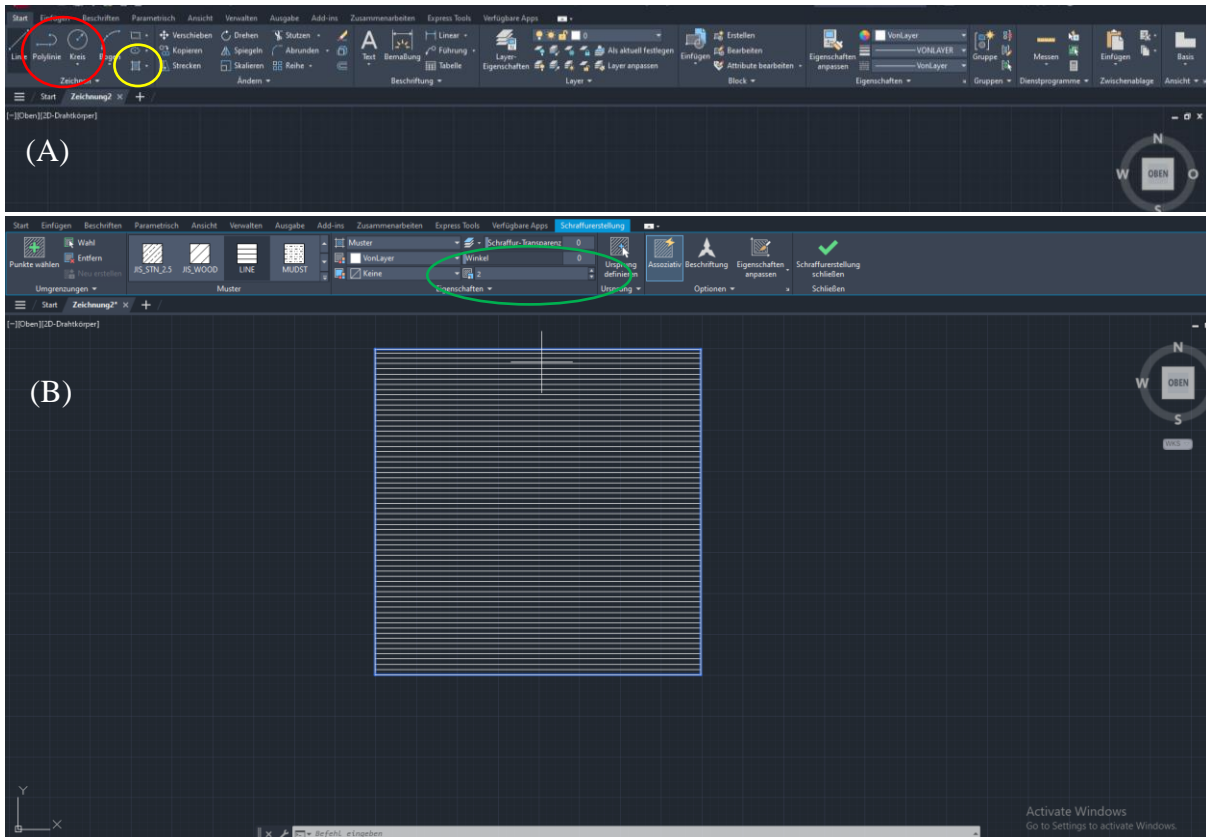


Figure15: (A) AutoCAD software tools. In red circle are Polylinie and Kreis. In yellow circle is hatch tool. (B) AutoCAD hatch tool. In green circle is density of lines adjustment.

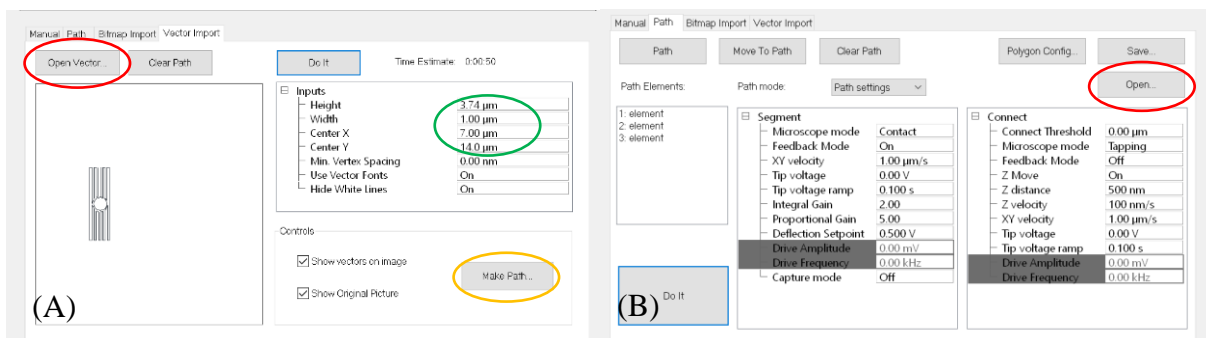


Figure 16: (A) NanoMan vector import. First open Vector (red circle), then adjust size and position (green circle), then make path (yellow circle). (B) nanoMan path. Open path (red circle)

#### 4.2.2 Testing out Patterns

The first pattern testing can be seen in Figure 17. Patterns from AutoCAD as well as patterns made in nanoMan were used. The cut made in AutoCAD was a rectangular shape containing two lines. The middle should not be cut. The patterns in nanoMan were one rectangular shape with a circle in the middle, a flower like shape and a circular shape. These patterns contained a lot of individual lines due to making them in nanoMan. Every time the direction changes a new line starts. (Figure 17 (A)) The patterns were cut one after another.

Patterns consisting of more than one line were apparently harder to execute, seen by missing cuts. The rounded cuts caused some part of the graphite to roll up, probably due to tension release. (Figure 17 (B)) Patterns made directly in nanoMan are more difficult to make for more advanced shapes. The pattern consists of a lot of individual lines that are hard to place exactly where they should be. For that reason, only patterns from AutoCAD are used from now on for everything except one line cuts.

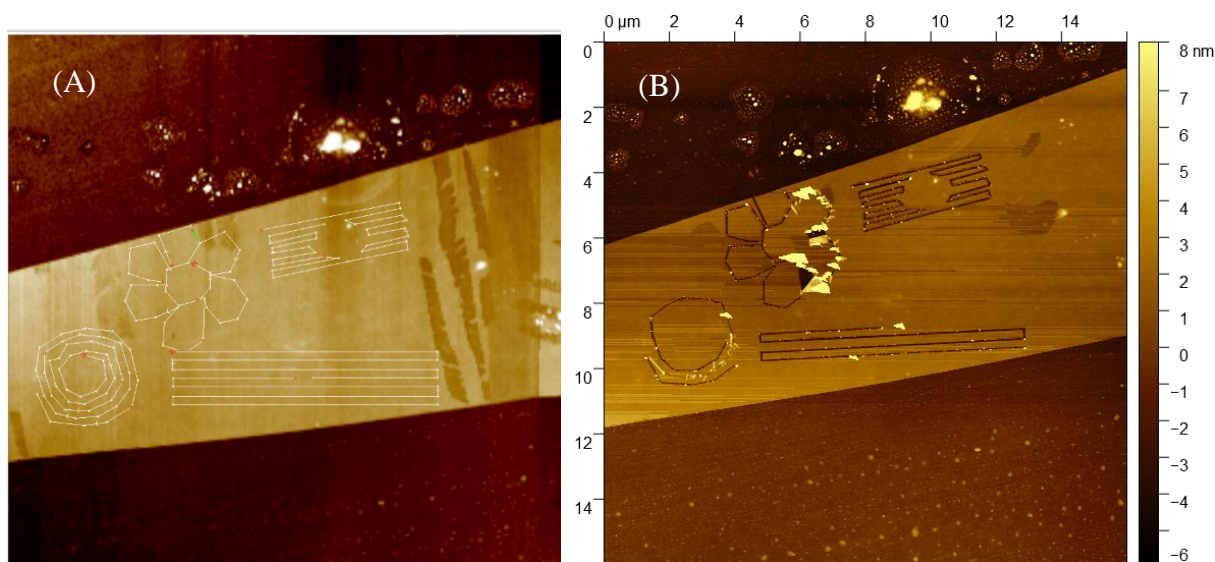


Figure 17: (A) Wanted pattern cuts. (B) Pattern cuts outcome.

In the next test a pattern for a rectangular shape was tested. It consisted of one line, which went from the outside to the inside. The pattern was cut twice in two individual runs. Before cutting the shape, a test cut was made in the same run. (Figure 18 (A)) This was made because of the difficulties in the cuttings that were observed before. In those the first line in the individual patterns often did not cut.

The patterns did cut but the test cut in the second try did not cut. Because of the cutting direction being outside to inside, the graphite started rolling up during the cut. (Figure 18 (B)) For that reason, the same pattern was tested again, but from the inside to the outside, which can be seen in the next test.

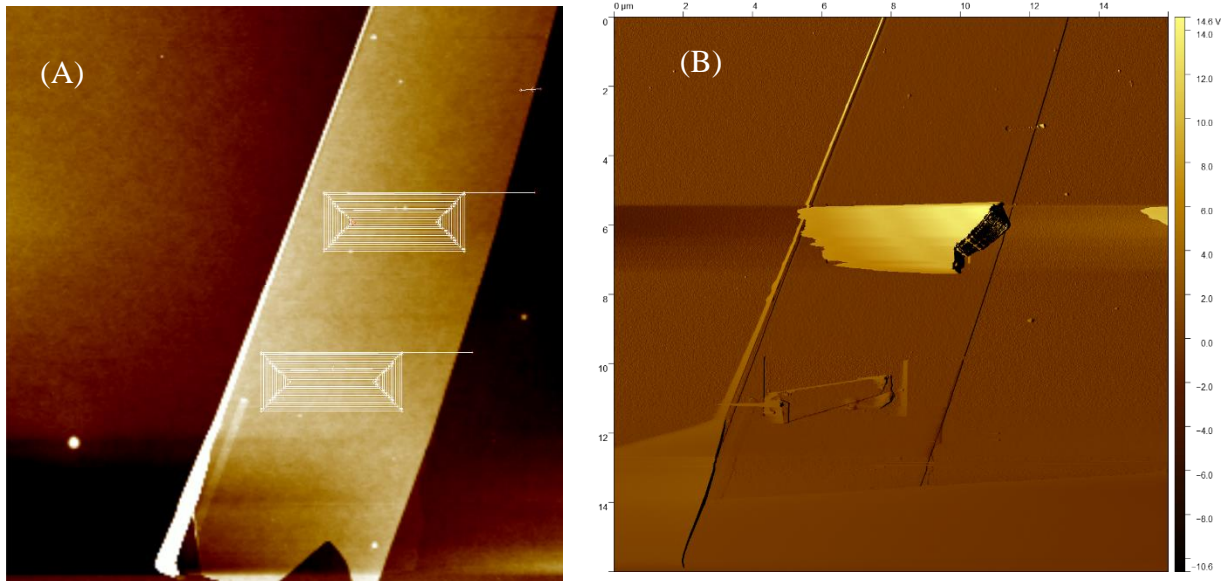


Figure 18: (A) Wanted pattern cuts. (B) Pattern cuts outcome.

In the next test two rectangular shapes and one shape for cutting a circle were tested. The patterns were cut individually and with a test cut as the first cut, like in the test before. The first rectangular shape is the same as in the test before, but with inversed cutting direction. The second pattern was one connected line, which went up and down. The third pattern consisted of one circle on the inside, which split up into individual lines, and one connected line around it. The line around was in rectangular shape and went up and down. (Figure 19 (A))

The first pattern went fine and no tension release by rolling up could be seen. In the second pattern the test cut did not show up this time, but the pattern was successful. In the third pattern

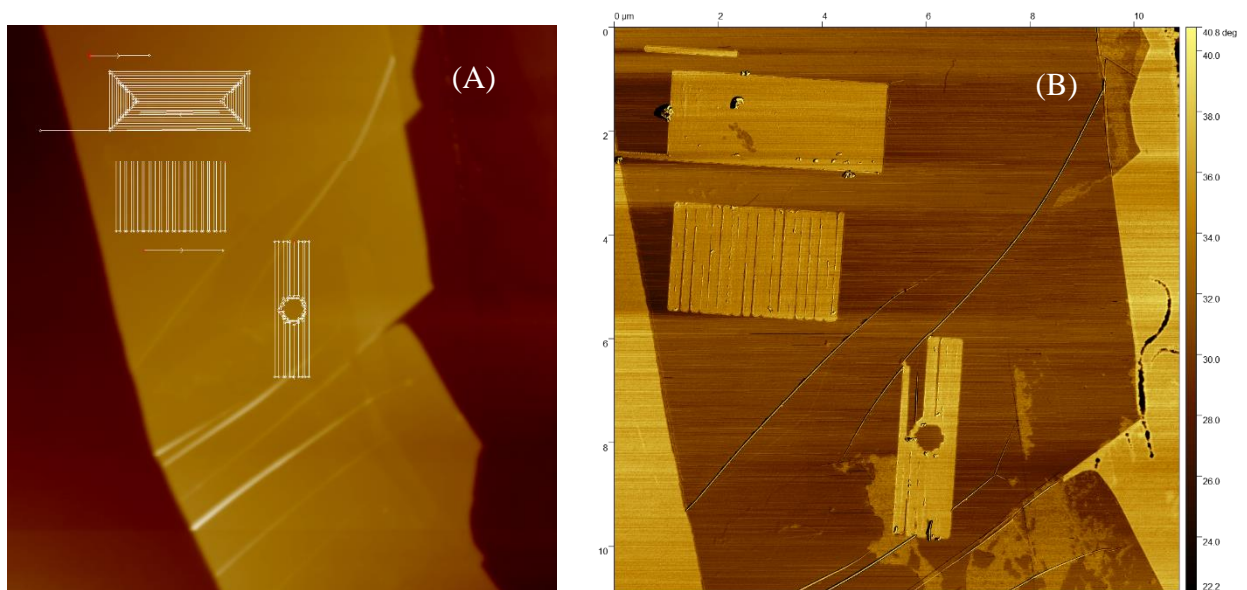


Figure 19: (A) Wanted pattern cuts. (B) Pattern cuts outcome

no test cut showed up and part of the rectangular line did not cut. This was probably due to the surface of the flake not being flat. (Figure 19 (B))

In the last test a hatched pattern and circle cut out was tested again. Every pattern was cut individually. The hatched pattern consisted of a circle in the inside and the hatching around it. The hatched pattern from AutoCAD translated in nanoMan resulted in every hatch line being an individual line to cut. The circle cut out pattern was a circle on the inside and a rectangle on the outside where the lines went up and down. It was tested out twice. In the second try of the pattern, it was cut two times in two individual runs. (Figure 20 (A))

The hatched pattern succeeded but was taking a long time, due to the number of individual lines. The circle pattern cut well. In the second test of that pattern the circle on the inside seems less clean. (Figure 20 (B))

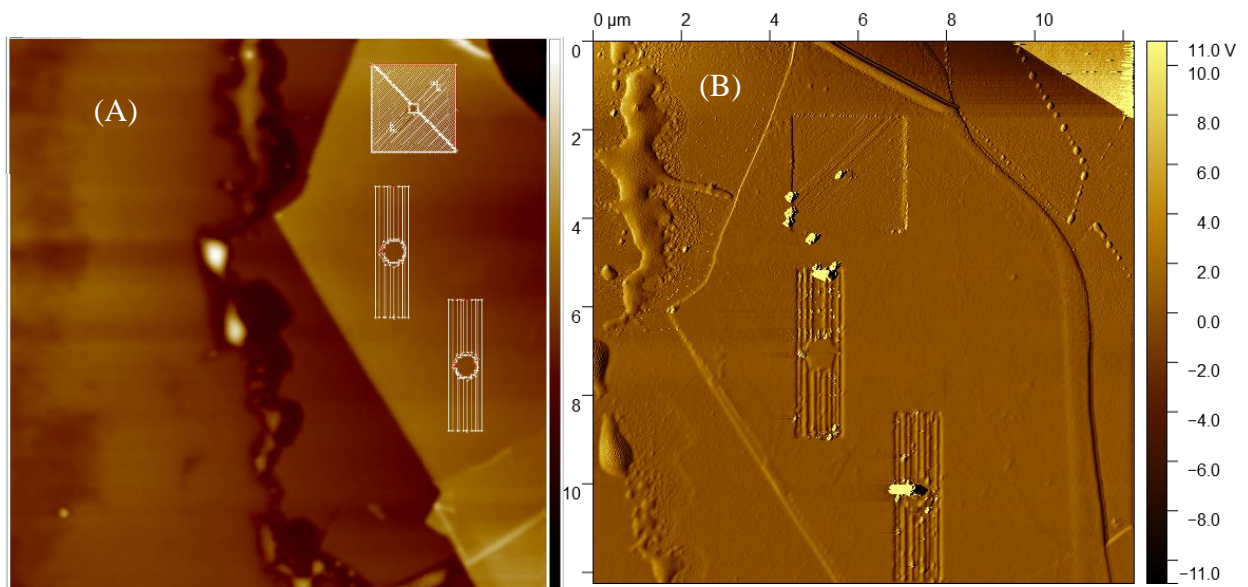


Figure 20: (A) Wanted pattern cuts. (B) Pattern cuts outcome

### 4.3 Picking up and dropping after AFM cutting

In theory the oxide residue that can be seen after a cut should not be picked up.<sup>18</sup> Here it was tested out with only the stamp for pickup. After the drop down of the flake the chip was cleaned from the rest of the PC from the stamp. This was first made by cleaning with chloroform for 5 min and after that it was cleaned in an annealer.

The cuts were visibly cleaner, and no oxide residue was left. There is still dirt on the flake that can result from the PC not cleaned well. It could also be because of dirt on the chip it was dropped on.

Another important thing that was noticed is that samples, which were cut from outside to inside, after picking up and dropping down, were visibly different to them before the process. During the picking up process, the flake probably moved. That is why some cuts were getting smaller or visibly disappeared and on the end of the cuts movement in the graphite appeared. (Figure 21) In the picked up and dropped down flake with only cuts in the inside less moving can be seen. (Figure 22) For cutting gates that will be used in devices, made by picking and dropping them, only cuts completely in the inside of the flake should be used to prevent the cuts from moving.

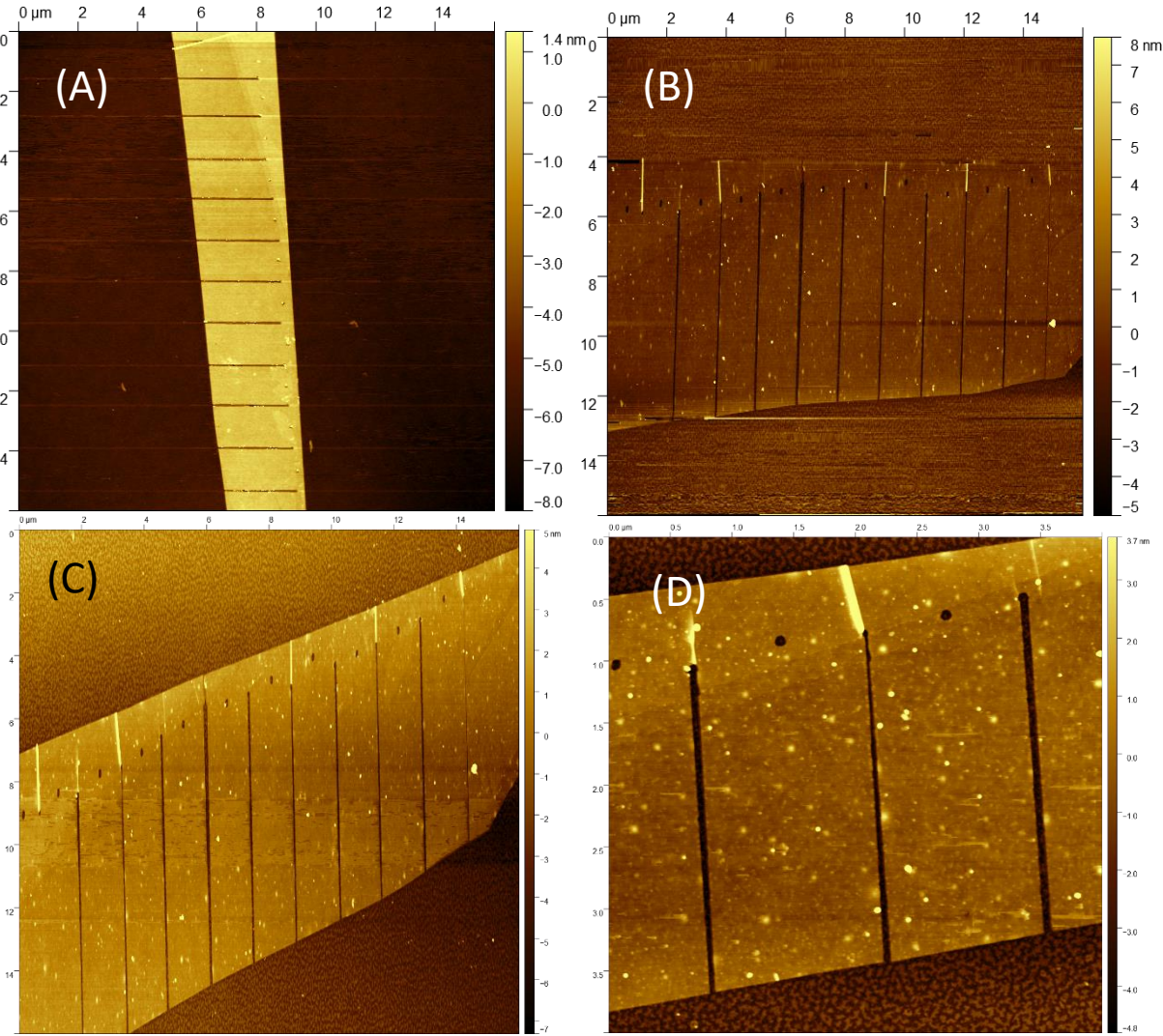


Figure 21: (A) Image before Pickup (B) Image after cleaning with chloroform (C) Image after cleaning in annealer (D) Zoom in on cuts 2-4.

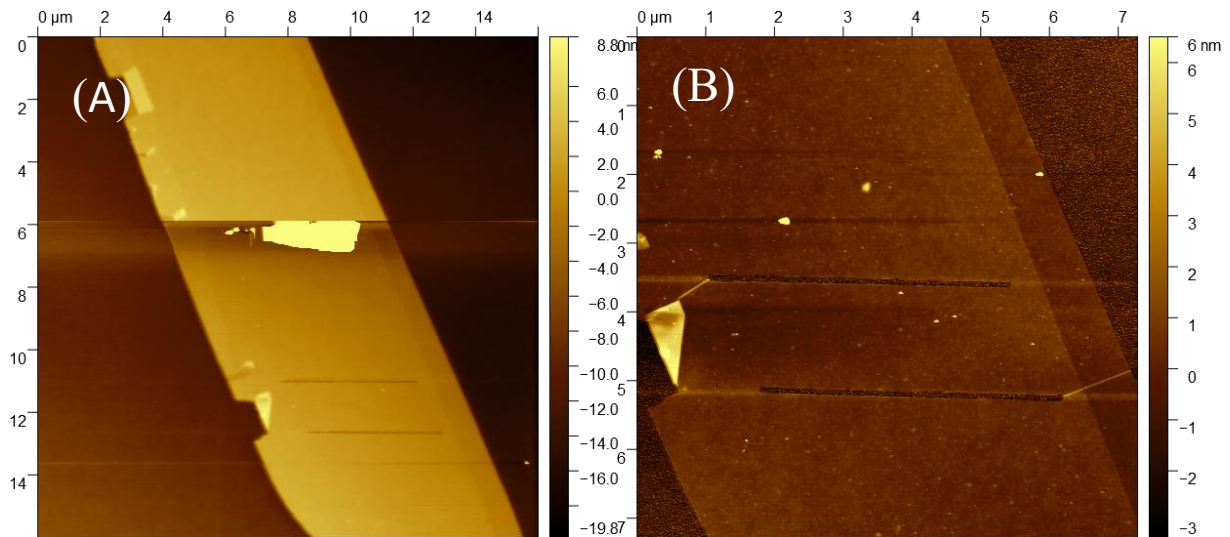


Figure 22: (A) Image before pickup (B) image after annealing.

## 5 Conclusion and Outlook

The original parameters were good, and cuts succeeded. The humidity should not go above 60 % to prevent bubbles to appear. It is difficult to predict the exact width of the cut due to a mix of parameters that come into play. For around 50 percent humidity cuts widths between 90 and 260 nm have been observed.

Patterned cuts should be made using AutoCAD. For patterned cuts one connected line cuts are the secure way to cut. In general, it is better to do a test cut. This prevents not cutting a pattern, because of the problem of not cutting the first line. To prevent tension release in form of graphite rolling up, only straight lines instead of curves should be used. And for a spiral cutting method one should only cut from the inside to the outside.

The self cleaning succeeded, and the cuts were clean. Cuts should be only in the inside of the flake, if used in a device.

In the future different things could be interesting to explore. For now, all cuts that were made, cut completely through the graphite. It would be interesting to test cutting in different depths. While testing out the system it happened that cuts with the exact same parameters sometimes cut and sometimes did not cut. This should be continued to explore. The cuts were only tested on graphite exfoliated on non etched chips. To test out if there is a difference between graphite exfoliated on etched chips could be interesting.

In the context of this work, the method was only tested regarding to use them in gates. In the future it could be interesting to try cutting hBN as well and test the application of that.

## 6 Bibliography

1. Novoselov, K. S. *et al.* Electric Field Effect in Atomically Thin Carbon Films. *Science* **306**, 666–669 (2004).
2. Castro Neto, A. H., Guinea, F., Peres, N. M. R., Novoselov, K. S. & Geim, A. K. The electronic properties of graphene. *Rev. Mod. Phys.* **81**, 109–162 (2009).
3. Sarma, S. D., Adam, S., Hwang, E. H. & Rossi, E. Electronic transport in two dimensional graphene. *Rev. Mod. Phys.* **83**, 407–470 (2011).
4. Novoselov, K. S. *et al.* Two-dimensional gas of massless Dirac fermions in graphene. *Nature* **438**, 197–200 (2005).
5. Zhang, Y., Tan, Y.-W., Stormer, H. L. & Kim, P. Experimental observation of the quantum Hall effect and Berry’s phase in graphene. *Nature* **438**, 201–204 (2005).
6. Gusynin, V. P. & Sharapov, S. G. Unconventional Integer Quantum Hall Effect in Graphene. *Phys. Rev. Lett.* **95**, 146801 (2005).
7. Katsnelson, M. I., Novoselov, K. S. & Geim, A. K. Chiral tunneling and the Klein paradox in graphene. *Nat. Phys.* **2**, 620–625 (2006).
8. Zhang, Y. *et al.* Direct observation of a widely tunable bandgap in bilayer graphene. *Nature* **459**, 820–823 (2009).
9. Rong, Z. Y. & Kuiper, P. Electronic effects in scanning tunneling microscopy: Moiré pattern on a graphite surface. *Phys. Rev. B* **48**, 17427–17431 (1993).
10. Bistritzer, R. & MacDonald, A. H. Moiré bands in twisted double-layer graphene. *Proc. Natl. Acad. Sci.* **108**, 12233–12237 (2011).
11. Cao, Y. *et al.* Unconventional superconductivity in magic-angle graphene superlattices. *Nature* **556**, 43–50 (2018).
12. Cao, Y. *et al.* Correlated insulator behaviour at half-filling in magic-angle graphene superlattices. *Nature* **556**, 80–84 (2018).
13. Díez-Mérida, J. *et al.* Symmetry-broken Josephson junctions and superconducting diodes in magic-angle twisted bilayer graphene. *Nat. Commun.* **14**, 2396 (2023).

14. Wang, P., Jia, C., Huang, Y. & Duan, X. Van der Waals Heterostructures by Design: From 1D and 2D to 3D. *Matter* **4**, 552–581 (2021).
15. Mayorov, A. S. *et al.* Micrometer-Scale Ballistic Transport in Encapsulated Graphene at Room Temperature. *Nano Lett.* **11**, 2396–2399 (2011).
16. Dean, C. R. *et al.* Boron nitride substrates for high-quality graphene electronics. *Nat. Nanotechnol.* **5**, 722–726 (2010).
17. Roy, S. *et al.* Structure, Properties and Applications of Two-Dimensional Hexagonal Boron Nitride. *Adv. Mater.* **33**, 2101589 (2021).
18. Cohen, L. A. *et al.* Nanoscale electrostatic control in ultraclean van der Waals heterostructures by local anodic oxidation of graphite gates. *Nat. Phys.* (2023) doi:10.1038/s41567-023-02114-3.
19. Huang, Y. *et al.* Reliable Exfoliation of Large-Area High-Quality Flakes of Graphene and Other Two-Dimensional Materials. *ACS Nano* **9**, 10612–10620 (2015).
20. Blake, P. *et al.* Making graphene visible. *Appl. Phys. Lett.* **91**, 063124 (2007).
21. *Functional nanostructures: processing, characterization, and applications.* (Springer, 2008).
22. Dimension Icon User Guide. *Dimension Icon User Guide* [https://www.nanophys.kth.se/nanolab/afm/icon/bruker-help/DIcon\\_webhelp\\_Left.htm#CSHID=Cover%2520page.htm|StartTopic=Content%2FCover%2520page.htm|SkinName=BrukerSkin](https://www.nanophys.kth.se/nanolab/afm/icon/bruker-help/DIcon_webhelp_Left.htm#CSHID=Cover%2520page.htm|StartTopic=Content%2FCover%2520page.htm|SkinName=BrukerSkin) (2023). (Last visited on 27.09.2023)
23. Li, H. *et al.* Electrode-Free Anodic Oxidation Nanolithography of Low-Dimensional Materials. *Nano Lett.* **18**, 8011–8015 (2018).
24. Han, W., Mathew, P. T., Kolagatla, S., Rodriguez, B. J. & Fang, F. Toward Single-Atomic-Layer Lithography on Highly Oriented Pyrolytic Graphite Surfaces Using AFM-Based Electrochemical Etching. *Nanomanufacturing Metrol.* **5**, 32–38 (2022).
25. Nanoworld Innovative Technologies. *Arrow<sup>TM</sup> NCPT* <https://www.nanoworld.com/tapping-mode-platinum-coated-afm-tip-arrow-ncpt>. (Last visited on 27.09.2023)

Hiermit erkläre ich, die vorliegende Arbeit selbständig verfasst zu haben und keine anderen als die in der Arbeit angegebenen Quellen und Hilfsmittel benutzt zu haben.

---

Ort, Datum der Abgabe

---

Unterschrift